Supporting information

High Performance All-Vanadate-Based Li-Ion Full Cell

*Jie Xu, Dongmei Zhang, Zongping Zhang, and Shibing Ni**

College of Materials and Chemical Engineering, Key Laboratory of Inorganic Nonmetallic Crystalline and Energy Conversion Materials, China Three Gorges University, Yichang, 443002, China.E-mail address: shibingni07@126.com;

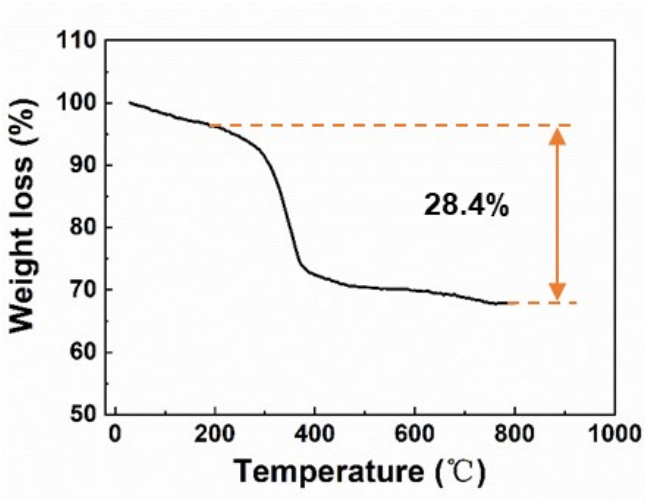

Figure S1. Thermogravimetric analysis of the LVO/NC PMSs.

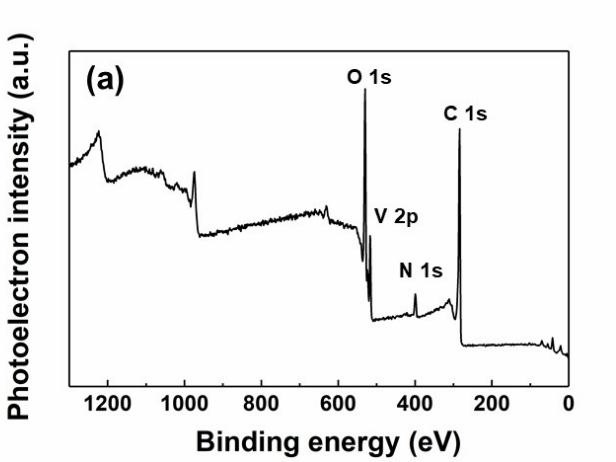

Figure S2. The survey XPS spectrum of the LVO/NC PMSs.

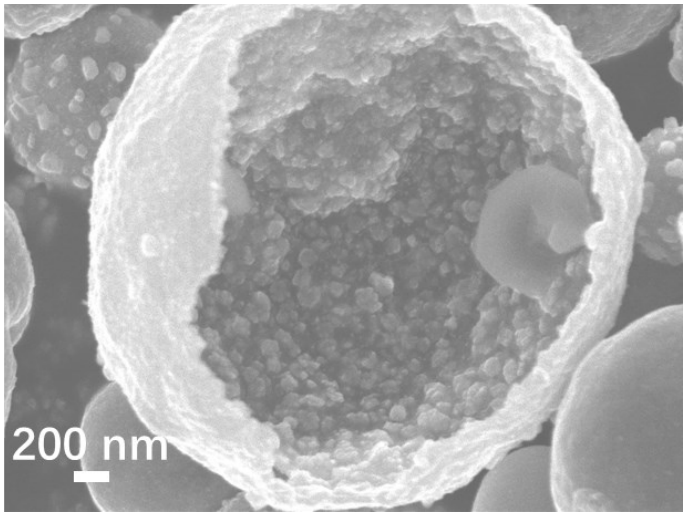

Figure S3. SEM image of a cracked LVO/NC PMS.

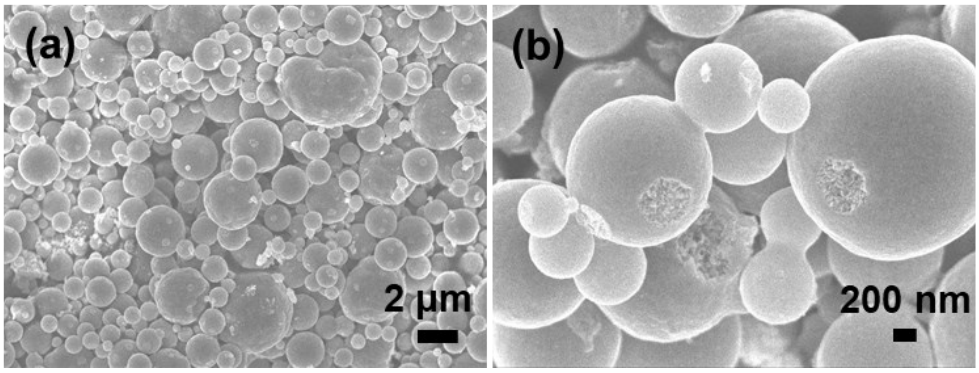

Figure S4. (a) Low and (b) high magnification SEM images of dense LVO/NC spheres obtained via concentrating the precursor solution to its 50% volume.

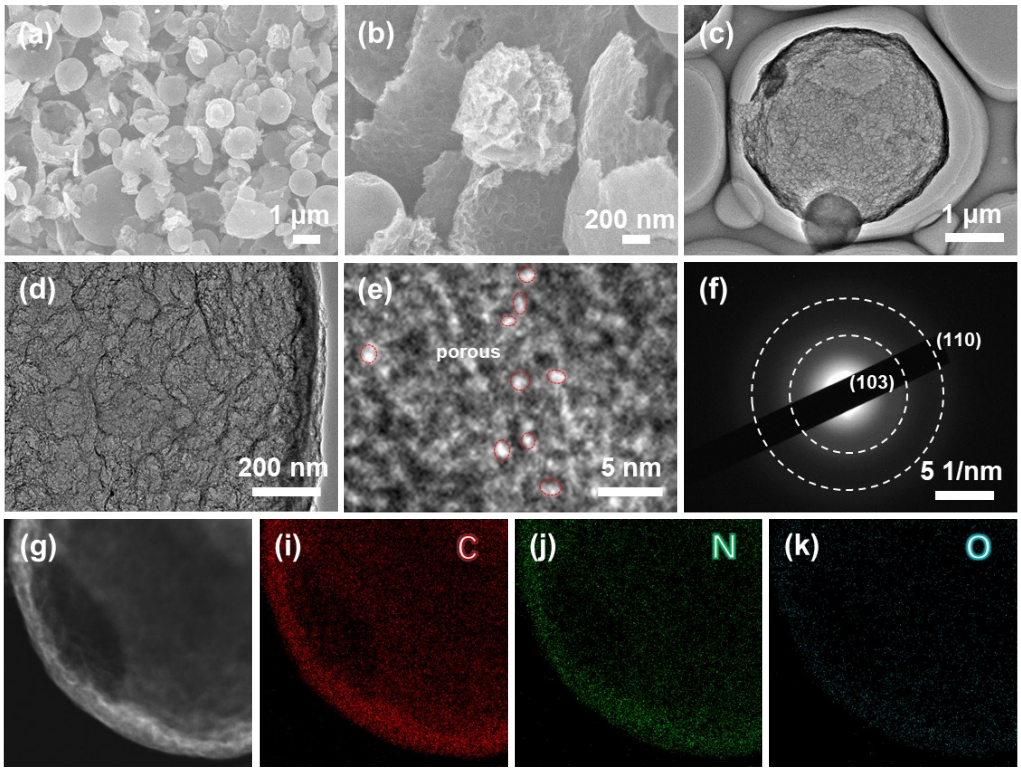

Figure S5. Morphological and microstructural characterizations of the products obtained via etching Li_3VO_4 in the LVO/NC PMS. (a, b) SEM and (c-e) TEM images. (f) SAED pattern. (g) Scanning TEM image and (i-k) the corresponding elemental mapping images of C, N, and O, respectively.

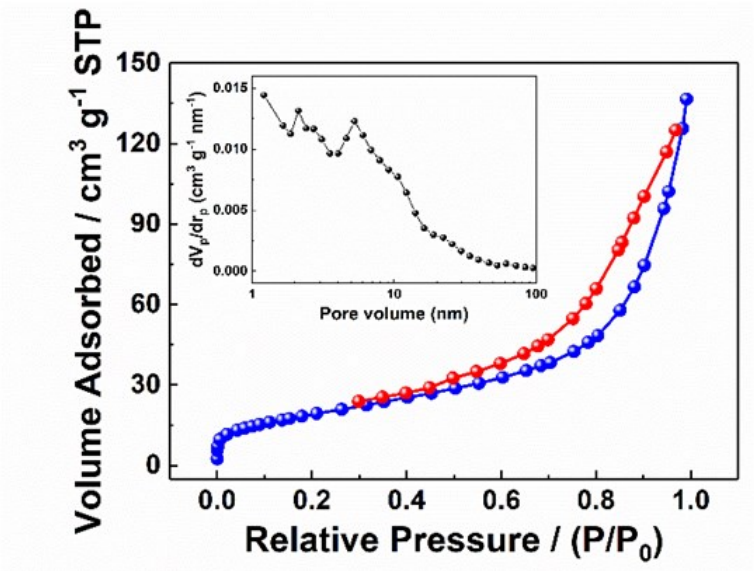

Figure S6. Nitrogen physisorption isotherms and (inset) pore size distributions of the LVO/NC PMSs.

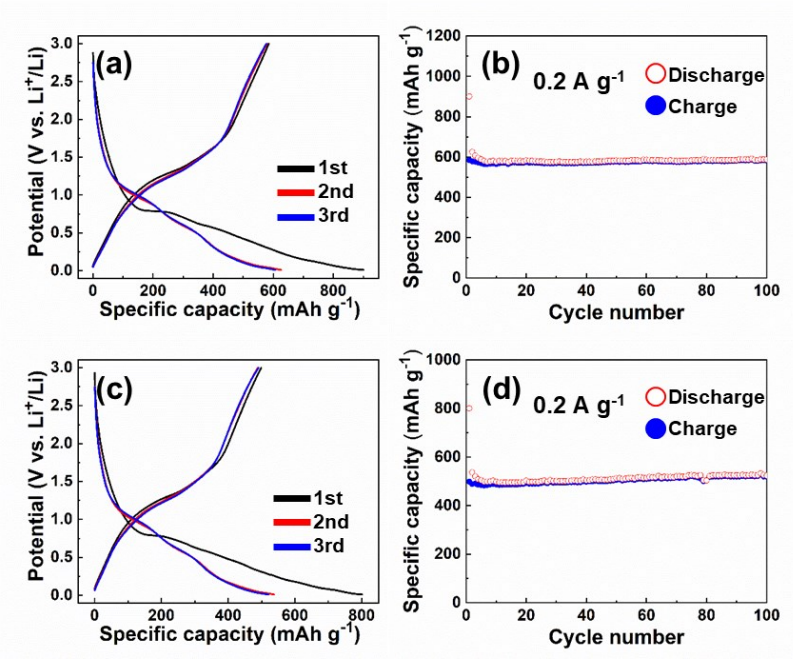

Figure S7. Electrochemical performance of the LVO/NC at specific current of 0.2 A g^{-1}. (a, b**)** for LVO/NC PMSs. (c, d**)** for dense LVO/NC spheres.

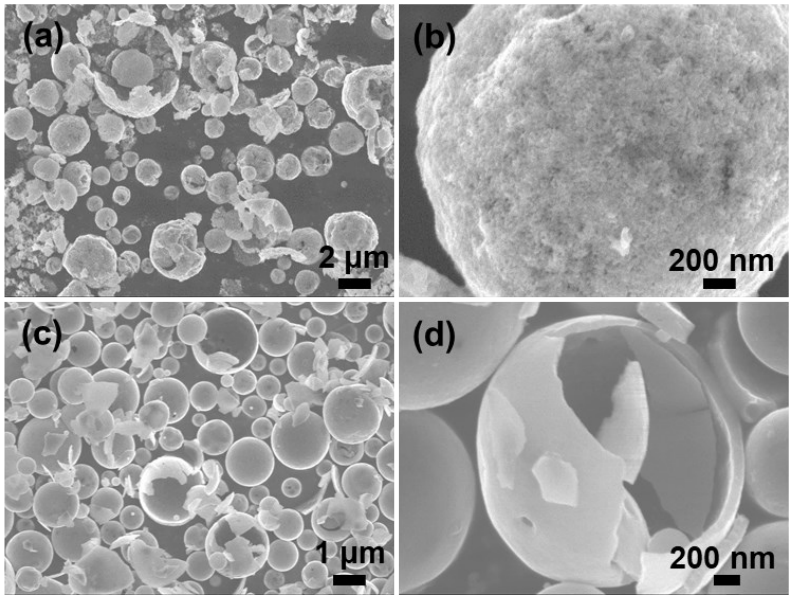

Figure S8. SEM images of LVO/NC spheres with different theoretical C content. (a, b**)** for 10%. (c, d) for 50%.

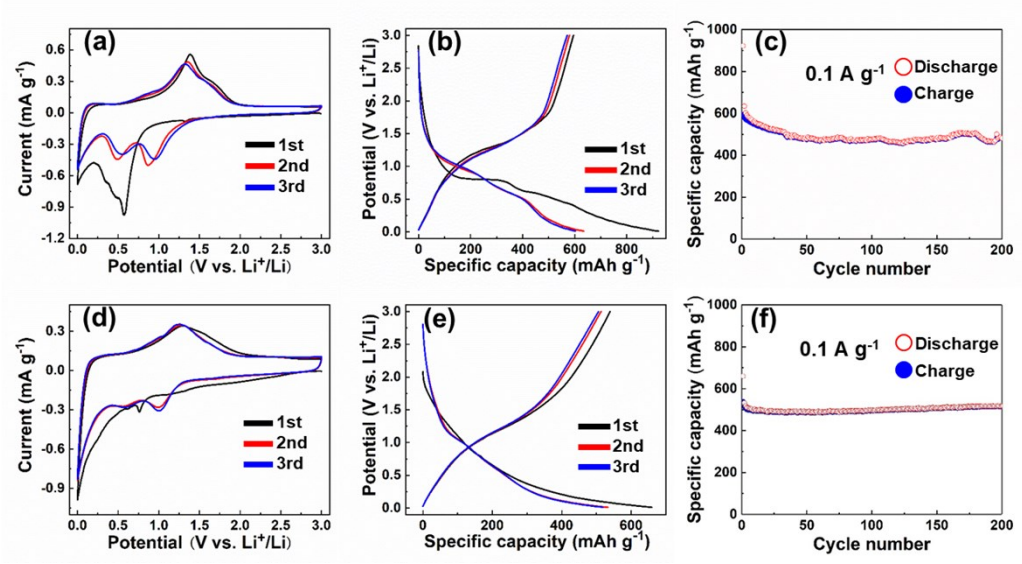

Figure S9. Electrochemical performance of the LVO/NC spheres with different theoretical C content. (a-c) for 10% C. (d-f) for 50% C.

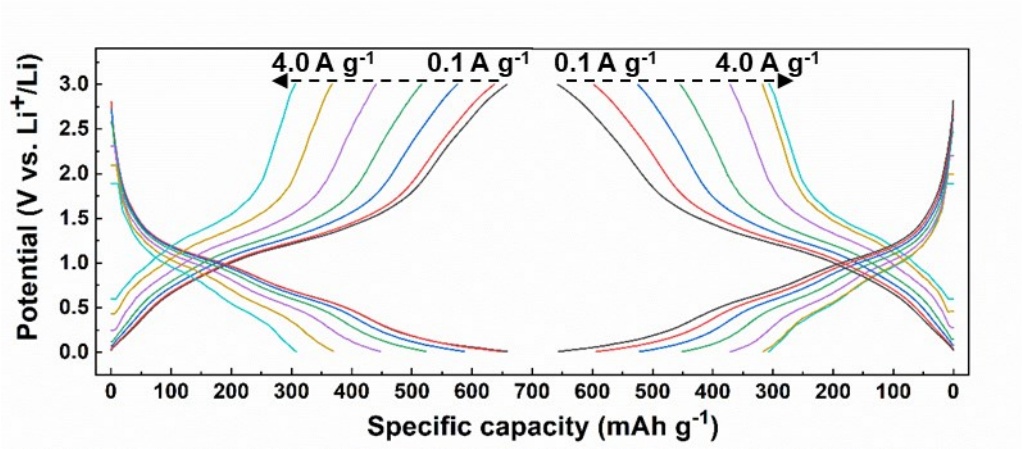

Figure S10. Representative charge/discharge curves in the second period rate performance testing in **Figure 4** d.

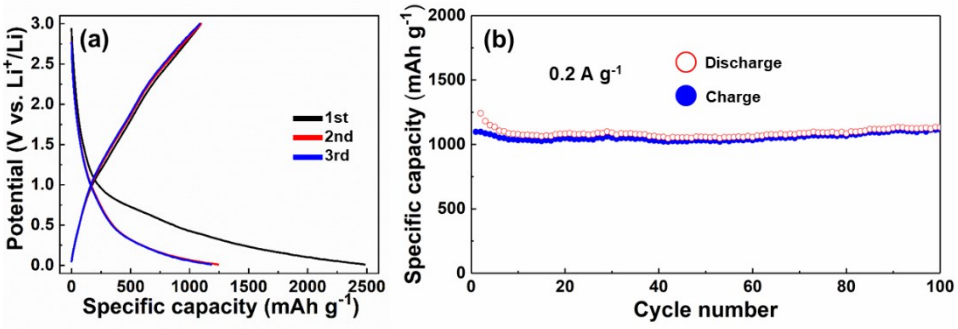

Figure S11. (a) The initial three charge/discharge curves and (b) cycle performance of NC obtained via etching Li_3VO_4 in the LVO/NC PMS.

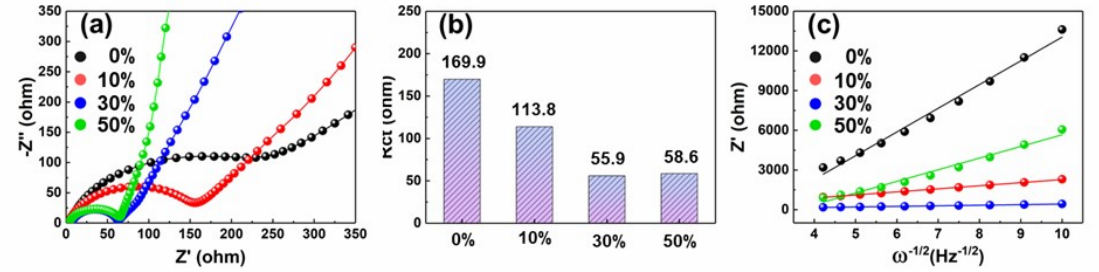

Figure S12. Electrochemical reaction kinetics of LVO/NC electrodes with different C component. (a) EIS spectra, (b) the fitted R_{ct} and (c) Nyquist plots of the real parts of the complex impedance versus $\omega^{-1/2}$.

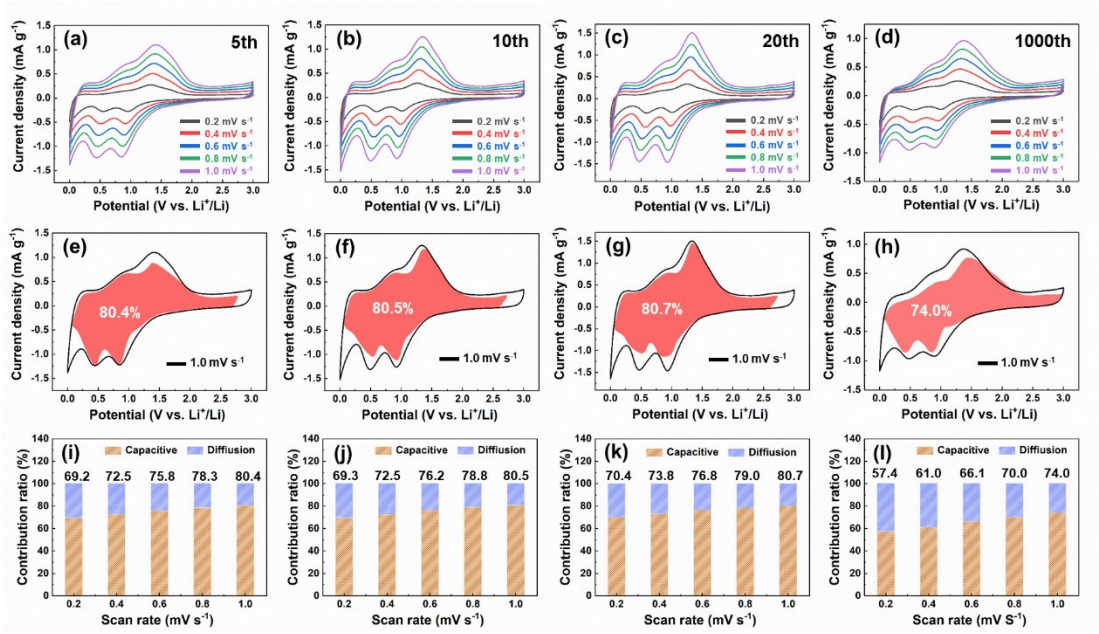

Figure S13. Li-ion storage electrochemistry of the LVO/NC PMSs. (a-d) CV curves at different scan rates; (e-h) fitted pseudocapacitive contribution in charge storage; (i-l) pseudocapacitive charge storage contribution vs. scan rate; (a, e, i) for electrode after 5 cycles, (b, f, j) for electrode after 10 cycles, (c, g, k) for electrode after 20 cycles, (d, h, l) for electrode after 1000 cycles.

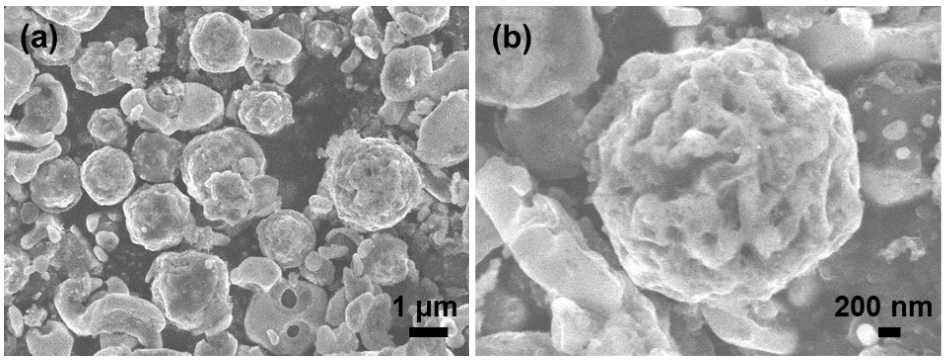

Figure S14. SEM images of LVP/C spheres with (a) low and (b) high magnification.

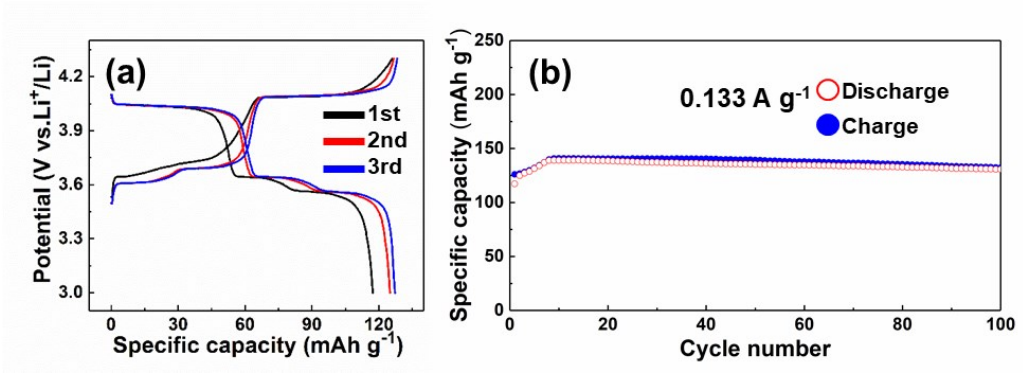

Figure S15. Electrochemical performance of LVP/C spheres with (a) the initial three charge/discharge curves and (b) Cycle performance at 1 C.

Table S1. The summarization of cycling performance of various LTO- and LVO-based full cells.

Material	Discharge current (mA g^{-1})	Capacity (mAh g^{-1})	Cycle number	Ref.
LVO//LFP	72	170	200	40
LVO//LNMO	1200	295	500	41
LVO//V_2O_5	1000	71.7	1500	63
LTO//LVP	65	104	30	69
LTO//LVP	650	120	300	71
LTO//LFP	17	68	50	73
LTO//LFP	34	83	300	74
LTO//LFP	~14	100	100	76
LTO//LFP	~500	122	200	77
LVO//LFP	400	350	100	78
LVO//LVP	1000	340.7	1000	This work